Institut de Physique Nucléaire de Lyon

Université Claude Bernard

IN2P3 - CNRS

LYCEN 2000/05
February 2000

Thermodynamical features of nuclear sources studied with INDRA

B. Borderie, et al., INDRA Coll.

International Symposium on Advances in Nuclear Physics
Bucarest (Roumanie) December 9-10, 1999
in Proceedings

43, Boulevard du 11 Novembre 1918 - 69622 VILLEURBANNE Cedex - France

THERMODYNAMICAL FEATURES OF NUCLEAR SOURCES STUDIED WITH INDRA

B. BORDERIE[1], CH.O. BACRI[1], R. BOUGAULT[2], A. CHBIHI[3], PH. CHOMAZ[3], M. COLONNA[4], J.D. FRANKLAND[1,3], A. GUARNERA[1], F. GULMINELLI[2], N. LE NEINDRE[2], M. PÂRLOG[5], M.F. RIVET[1], S. SALOU[3], G. TĂBĂCARU[1,5], L. TASSAN-GOT[1], J.P. WIELECZKO[3] G. AUGER[3], N. BELLAIZE[2], F. BOCAGE[2], B. BOURIQUET[3], R. BROU[2], P. BUCHET[6], J.L. CHARVET[6],, J. COLIN[2], D. CUSSOL[2], R. DAYRAS[6], N. DE CESARE[7], A. DEMEYER[8], D. DORÉ[6], D. DURAND[2], E. GALICHET[1,9], E. GENOUIN-DUHAMEL[2], E. GERLIC[8], S. HUDAN[3], D. GUINET[8], F. LAVAUD[1], P. LAUTESSE[8], J.L. LAVILLE[3], J.F. LECOLLEY[2], C. LEDUC[3], R. LEGRAIN[6], O. LOPEZ[2], M. LOUVEL[2], A.M. MASKAY[8], L. NALPAS[6], J. NORMAND[2], J. PÉTER[2], E. PLAGNOL[1], E. ROSATO[7], F. SAINT-LAURENT[3]*, J.C. STECKMEYER[2], B. TAMAIN[2], O. TIREL[3], E. VIENT[2], M. VIGILANTE[7], C. VOLANT[6], (INDRA COLLABORATION)

1 *Institut de Physique Nucléaire, IN2P3-CNRS, F-91406 Orsay Cedex, France.*
2 *LPC, IN2P3-CNRS, ISMRA et Université, F-14050 Caen Cedex, France.*
3 *GANIL, CEA et IN2P3-CNRS, B.P. 5027, F-14076 Caen Cedex, France.*
4 *Lab. Nat. del Sud, Via S. Sofia 44, I-95123 Catania, Italy.*
5 *National Institute for Physics and Nuclear Engineering, RO-76900 Bucharest-Măgurele, Romania.*
6 *DAPNIA/SPhN, CEA/Saclay, F-91191 Gif sur Yvette Cedex, France.*
7 *Dipartimento di Scienze Fisiche e Sezione INFN, Universiti Napoli 'Federico II", I-80126 Napoli, Italy.*
8 *Institut de Physique Nucléaire, IN2P3-CNRS et Université, F-69622 Villeurbanne Cedex, France.*
9 *Conservatoire National des Arts et Métiers, F-75141 Paris cedex 03.*

Vaporized and multifragmenting sources produced in heavy ion collisions at intermediate energies have been detected with the multidetector INDRA. The properties of such highly excited nuclear sources which undergo a simultaneous disassembly into particles (vaporization) are discussed in terms of thermal and chemical equilibrium at freeze-out. For multifragmenting sources which undergo a simultaneous disassembly into particles and fragments, properties of fragments are compared to different models assuming statistical fragment emission or spinodal instabilities. Experimental charge correlations for fragments show a weak but non ambiguous signal of the enhancement of events with nearly equal size fragments. Such a signal can be interpreted as a trace of spinodal instabilities.

*present address: DRFC/STEP, CEA/Cadarache, F-13018 Saint-Paul-lez-Durance cedex, France.

1 Introduction

The decay of highly excited nuclear systems through a simultaneous disassembly is, at present time, a subject of great interest in nucleus-nucleus collisions at intermediate energies. Although this process has been observed for many years, its experimental knowledge in the Fermi energy domain was strongly improved only recently with the advent of powerful 4π devices such as INDRA [1]. Well defined systems or subsystems which undergo vaporization or multifragmentation can be thus carefully selected.

To describe the simultaneous disassembly of highly excited nuclear sources produced in nucleus-nucleus collisions, many models presuppose that when they disintegrate these sources have achieved partial or complete thermodynamical equilibrium [2,3,4,5,6,7,8]. This hypothesis is essential if one wants to describe the sources and understand the generated mechanisms for disassembly as well as the properties by means of macroscopic variables such as temperature and related pressure and density. However such an assumption is *a priori* not obvious if we bear in mind the shortening of all time scales with respect to those involved at low and moderate excitation energies. The very fundamental questions of the degree of equilibrium reached before disassembly and of the mechanism responsible for disassembly can be only answered by confronting these models to complete data on the deexcitation of well identified nuclear sources.

2 Thermal and chemical equilibrium for vaporizing sources

Let us first report on a comparison of the properties of vaporized quasi-projectiles (QP), produced in binary dissipative collisions between ^{36}Ar and ^{58}Ni nuclei at 95 MeV/u incident energy [9], with a quantum statistical model describing a gas of fermions and bosons in thermal and chemical equilibrium which includes a final state volume interaction (van der Waals-like behavior) and side feeding [10,11].

These sources are very interesting because they represent an extreme deexcitation mode for very hot pieces of nuclear matter, close to the expectation of a supercritical nuclear gas [12,13]. In the model, to cover the experimental range in excitation energy per nucleon of the source (ε^*), the temperature had to be varied from 10 to 25 MeV. Isospin (N/Z) was fixed to 1, which is very close to the N/Z of the system. Finally the freeze-out density has been fixed to $\rho = \rho_0/3$, in order to reproduce the experimental ratio between the proton and alpha yields at ε^*=18.5 MeV.

Fig 1 shows the evolution of the chemical composition as a function of

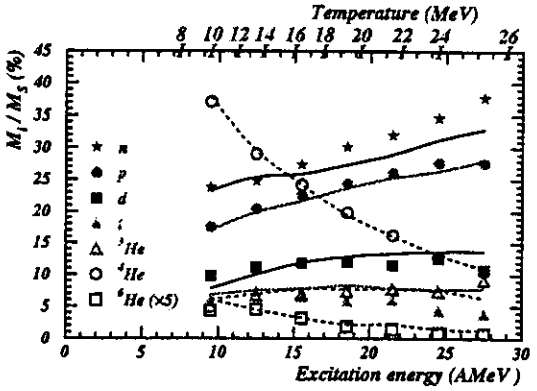

Figure 1. Composition of the QP as a function of its excitation energy. Symbols are for data while the lines (dashed for He isotopes) are the results of the model. The temperature values used in the model are also given. (from [11]).

excitation energy of the source; we observe an excellent agreement between data and model. Average kinetic energies of the different particles as well as second moments of the chemical composition are also well reproduced over the whole excitation energy range [11].

The scenario producing such sources may be the following: after an interaction time of around 40 fm/c (estimated from the time needed by the two nuclei to pass through each other), partners of collisions are on the way to thermalization. Then, due to the very high excitation energies involved, the partners start to dissociate and reach a density around $\rho = \rho_0/3$ within about 30 fm/c (see for example ref. [14,15]). Finally at low density and at very high temperatures in the supercritical region of the phase diagram [12,13], the emission properties of vaporized sources at freeze-out are fixed by thermodynamical equilibrium .

3 Experimental evidence for bulk effect in multifragmentation

Using the INDRA detector, multifragmenting fused systems have been carefully selected for two reactions leading to the same available excitation energy per nucleon ($\sim 7MeV$) : $^{129}Xe + ^{nat}Sn$ at 32 MeV/u and $^{155}Gd + ^{nat}U$ at 36 MeV/u. The selection was performed by examining the evolution of fragment kinematics as a function of the dissipated energy and loss of memory of the entrance channel [16,17].

Fig 2 shows that, for the two fused systems, we observe the same Z distribution for fragments while, as a consequence, the fragment multiplicities scale as the size of the total systems. This independence of the Z distribution, experimentally observed for the first time [16], can be considered as a strong

evidence for a bulk effect to produce fragments. It can be related to bulk instabilities in the liquid-gas coexistence region of nuclear matter (spinodal region) or perhaps simply taken as a signature of a full exploration of phase space for such heavy systems.

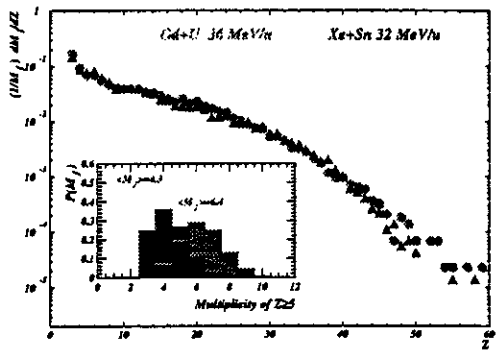

Figure 2. Experimental fragment multiplicity distributions and differential charge multiplicity distributions for the 32 MeV/u Xe+Sn (black histogram and triangles) and 36 MeV/u Gd+U (grey histogram and circles).

4 Comparison to models

Many theories have been developed to explain multifragmentation (see for example ref. [18] for a general review of models). Among the models some are related to statistical approaches whereas others, more ambitious, try to describe the dynamical evolution of systems, from the beginning of the collision between two nuclei to the fragment formation. In the latter, theoretical scenarios to be compared with experimental data are simulated (with approximations) via molecular dynamics, eventually including a stochastic implementation [19] or momentum fluctuations [20], or stochastic mean field approaches which account for the dynamics of the phase transition. It is this last type of approach that we shall first use for a comparison with our experimental observables. In simulations spinodal decomposition of hot and dilute nuclear systems are mimicked and, relative to the standard nuclear Boltzmann treatment, a powerful approximate tool is provided by the Brownian One-Body (BOB) dynamics [21,8]. The BOB dynamics introduces a noise by means of a brownian force in the mean field whenever the local conditions correspond to spinodal instability. Thus the magnitude of the force is adjusted to produce the same growth rate as the full Boltzmann-Langevin theory for the most unstable modes in nuclear matter prepared at the corresponding density and temperature [22].

In reference [16], it was shown that the multiplicity and charge distributions for both systems were correctly reproduced, but that the calculated fragment kinetic energies were too low. Since then two major improvements have been implemented in the simulations. Firstly, in deterministic or stochastic simulations, the collision term is assumed to be local in both space and time; this simplification is no more justified when fast unstable modes are present as in the spinodal region. Then quantal fluctuations connected with collisional memory effects are now taken into account with the determinant result of about doubling the overall amplitude of fluctuations [23]. Secondly the previous simulation method consisted in simply injecting the correct (classical) fluctuations when the system enters the spinodal region (Stochastic Initialisation Method) [24]. This method led to a damping of the fluctuations. The fragment formation time was thus artificially (and incorrectly) increased, leading to smaller kinetic energies due to the decrease with time of the radial expansion of the system. Then a better simulation method (BOB) was proposed [21,8] which takes into account the time dependence of the fluctuation source. This method is analogous to the Langevin treatment of Brownian motion.

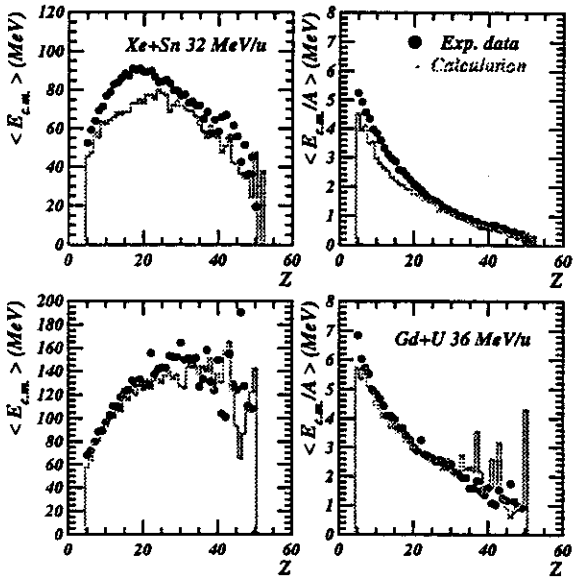

Figure 3. Experimental (points) and simulated (histograms) average fragment kinetic energies. Histograms are the calculated values when the thermal kinetic energy is added; indeed the introduced fluctuations act mostly on the configuration space but they do not provide a good description of fluctuations in momentum space. The results are for total energies on the left, and in MeV/u on the right.

The simulation (for head-on collisions, as fluctuations calculated for infinite matter can be rather safely extrapolated only to systems having a spherical symmetry) thus proceeds as follows [17]: the dynamics is followed through

a BNV/BOB simulation, up to the time where the fragments are formed and well separated. The fluctuating force starts acting at the time of maximum compression (25-30% higher than normal density) when local thermal equilibrium is fulfilled. Slightly after entering the spinodal region, the systems are in thermal equilibrium at low density (0.4 the normal density), with a temperature of 4 MeV. The radial velocity at the surface is rather large ~0.1c. When the fragments are well separated, they still bear an average excitation energy of ~3.2 MeV/u. Then the de-excitation of the hot primary fragments, whose mass accounts for 80% of the total system mass is followed through the evaporation part of the SIMON code. Finally the results are filtered to take into account the experimental set-up.

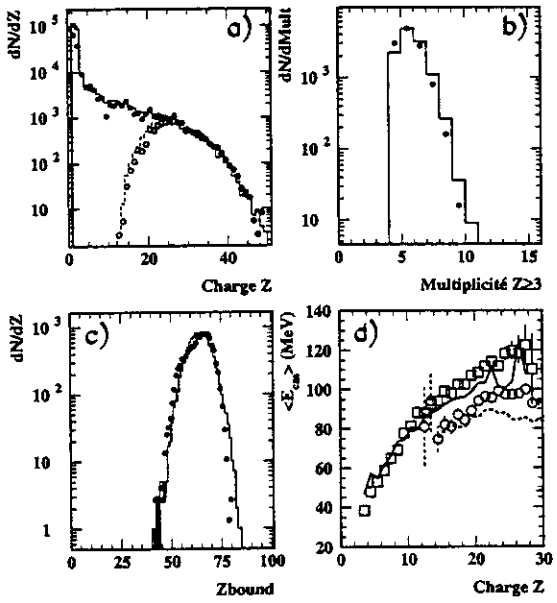

Figure 4. Experimental (points, open square and open points) and SMM simulations (histograms and full and dashed curves): a) fragment charge distrib., b) fragment multiplicity distrib., c) total charge into fragments Z_{bound}, d) average kinetic energies of fragments but the largest (squares and full curve) and of the largest (open circles and dashed curve) as a function of their Z. Inputs in SMM calculations are A=202, Z=85, excitation energy=5.0 AMeV (thermal)+0.6 AMeV (radial expansion) and partitions are fixed at 1/3 the normal density (from [27]).

Calculated multiplicity and charge distributions of fragments well match the experimental ones and more detailed comparisons on the charge distributions of the three largest fragments display the same excellent agreement [17]. Finally the most crucial test is performed on the fragment kinetic energies. Figure 3 shows that the simulations now correctly reproduce the fragment energies for the Gd+U system. For Xe+Sn, the calculated energies fall within 20% of the measured values, which is satisfactory if one remembers that there

were no adjustable parameters in the simulation.

A very good agreement with experimental data is also observed when they are compared to the statistical model SMM [2,25,26,27,28]. Figure 4 shows this comparison for the Xe+Sn system at 32 MeV/u. For Gd+U the thermal part of the excitation energy is also fixed at 5.0 AMeV to well reproduce experimental data. However in this case the dynamical phase of the reaction is ignored and parameters such as the mass and charge of the multifragmenting system, its excitation energy, its volume (or density) and the added radial expansion have to be backtraced to the experimental data.

5 Charge correlation of fragments and spinodal decomposition

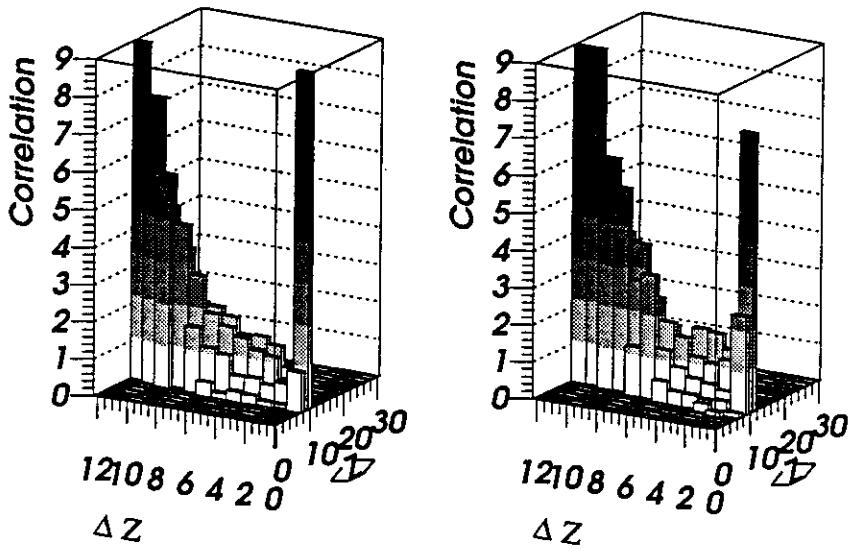

Figure 5. Fragment charge correlations for the reaction $^{129}Xe+^{nat}Sn$ at 32 MeV/u: Comparison between experiment (left) and BOB calculations (right) for fragment multiplicity equal to 6 (from [29]).

To put ultimate constraints on models, we can and should also compare fragment correlations in events (fragment size [29] and fragment reduced velocities [25]). In particular, for fragment size correlations, if spinodal instabilities

occur the most unstable modes present in the spinodal region are predicted to favor "primitive" partitions of equal size fragments (Z:10-15) [24]. But this simple picture is blurred by several effects: the beating of different modes, the coalescence of the "primitive " fragments and the finite size of the system and consequently experimental Z distributions (see fig 2) do not present any visible enhancement around Z=10-15. Then how to search for a possible very weak "fossil" signature of spinodal decomposition? A few years ago a new method called higher order charge correlations was proposed in [30]. To search for very weak signals, all fragments in one event (average fragment charge Z and the standard deviation per event ΔZ) are used to build the charge correlation for each fragment multiplicity. Due to statistics in experiments this method could be only applied on the Xe+Sn system [29]. A signal is observed for the different multiplicities from 3 to 6. An example of the observed experimental correlations is shown in figure 5 (left part). Note that if we enlarge our data sample to the very dissipative collisions (dominated by binary collisions) the signal is no more present. Concerning the models we again observe an impressive agreement of the BNV/BOB simulation (simulated events are filtered to take into account the experimental set-up) with the data (right part). Conversely results on charge correlations built with SMM events do not show any signal for an enhancement of events with equal size fragments.

6 Conclusions

Thermal and chemical equilibrium for a gas phase composed of fermions and bosons well reproduces the properties of vaporized sources experimentally selected with INDRA. Inclusion of a van der Waals-like behavior was found decisive to obtain the observed agreement. Concerning heavy fused sytems formed in the Fermi energy domain, a "fossil" signature of spinodal decomposition as the mechanism responsible for multifragmentation of such systems is probably observed for the first time. It consists in an enhancement of events with equal size fragments. A full dynamical model including also the dynamics of spinodal instabilities reproduces impressively all the experimental observables. However, except the weak "fossil" signal and the precise description at freeze-out (velocity correlations for fragments) [25], statistical models, when adding a radial expansion, reproduce also very well the experimental observables. This fact seems to be a strong indication that dynamical instabilities responsible for mutifragmentation lead to an exploration of practically all the phase space.

References

1. J. Pouthas *et al.*, (INDRA coll.), *Nucl. Instrum. Methods* A **357**, 418 (1995).
2. J. Bondorf et al., *Phys. Rep.* **257**, 133 (1995) and references therein.
3. D.H.E. Gross, *Rep. Prog. Phys.* **53**, 605 (1990) and references therein.
4. A. Z. Mekjian, *Phys. Rev.* C **17**, 1051 (1978).
5. H. Stöcker and W. Greiner, *Phys. Rep.* **5**, 277 (1986), J. Konopka et al., *Phys. Rev.* C **50**, 2085 (1994).
6. W. A. Friedman, *Phys. Rev.* C **42**, 667 (1990).
7. B. Borderie, *Ann. Phys. Fr.* **17**, 349 (1992), P. Abgrall et al., *Phys. Rev.* C **49**, 1040 (1994).
8. A. Guarnera et al., *Phys. Lett.* B **403**, 191 (1997).
9. M.F. Rivet et al., (INDRA coll.) *Phys. Lett.* B **388**, 219 (1996).
10. F. Gulminelli and D. Durand, *Nucl. Phys.* A **615**, 117 (1997).
11. B. Borderie *et al.*, (INDRA coll.), *Eur. Phys. J.* A **6**, 197 (1999), *Phys. Lett.* B **388**, 224 (1996).
12. H. R. Jaqaman et al., *Phys. Rev.* C **29**, 2067 (1984).
13. J. N. De et al., *Phys. Rev.* C **55**, 1641 (1997).
14. D. Vautherin et al., *Phys. Lett.* B **191**, 6 (1987).
15. L. Vinet et al., *Nucl. Phys.* A **468**, 321 (1987).
16. M.F. Rivet et al., (INDRA collaboration), *Phys. Lett.* B **430**, 217 (1998).
17. J.D. Frankland, thèse, Université Paris XI Orsay, 1998, IPNO-T-98-06.
18. L. G. Moretto and G. J. Wozniak, *Ann. Rev. of Nuclear and Particle Science* **43**, 379 (1993) and references therein.
19. A.Ono an H. Horiuchi, *Phys. Rev.* C **53**, 2958 (1996).
20. Y. Sugawa and H. Horiuchi, *Phys. Rev.* C **60**, 064607-1 (1999) and references therein.
21. Ph. Chomaz et al., *Phys. Rev. Lett.* **73**, 3512 (1994).
22. Ph. Chomaz, *Ann. Phys. Fr.* **21**, 669 (1996).
23. S. Ayik and J. Randrup, *Phys. Rev.* C **50**, 2947 (1994).
24. A. Guarnera et al., *Phys. Lett.* B **373**, 267 (1996).
25. S. Salou, *thèse*, Université de Caen, GANIL T 97 06.
26. R. Bougault et al., (INDRA coll.) in *Proc. of the XXXV Int. Winter Meeting on Nuclear Physics*, Bormio, Italy (1997), ed I. Iori, Ricerca scientifica ed educazione permanente, page 251.
27. N. Le Neindre, *thèse*, Université de Caen, LPCC T 99 02.
28. Ch. O. Bacri, private communication
29. G. Tăbăcaru, *thèse*, Université Paris XI Orsay, in preparation.
30. L. G. Moretto et al.,*Phys. Rev. Lett.* **77**, 2634 (1996).